VIP Sequence-Defined Polymers Very Important Paper

DOI: 10.1002/ange.201310937

An Efficient and Modular Route to Sequence-Defined Polymers Appended to DNA**

Thomas G. W. Edwardson, Karina M. M. Carneiro, Christopher J. Serpell, and Hanadi F. Sleiman**

Abstract: *Inspired by biological polymers, sequence-controlled synthetic polymers are highly promising materials that integrate the robustness of synthetic systems with the information-derived activity of biological counterparts. Polymer–biopolymer conjugates are often targeted to achieve this union; however, their synthesis remains challenging. We report a stepwise solid-phase approach for the generation of completely monodisperse and sequence-defined DNA–polymer conjugates using readily available reagents. These polymeric modifications to DNA display self-assembly and encapsulation behavior—as evidenced by HPLC, dynamic light scattering, and fluorescence studies—which is highly dependent on sequence order. The method is general and has the potential to make DNA–polymer conjugates and sequence-defined polymers widely available.*

The control of monomer sequence in synthetic polymers is a major challenge for modern polymer chemistry. The key processes in molecular biology are executed by proteins and nucleic acids—natural sequenced polymers capable of storing data and generating complex structure and function. Synthetic sequence-controlled polymers may find applications in the fields of data storage and biomedicine, and in the creation of materials with precisely tunable bulk properties and function.[1] To date, a number of strategies have been proposed for the synthesis of sequence-defined polymers,[2] ranging from solid-phase sequential addition of monomers through peptide coupling or other coupling reactions,[3] to biomolecule-templated polymerization,[4] to control of the polymerization mechanism such that addition of a one or few monomers to a growing polymer chain is possible.[5] Solid-phase synthesis is especially powerful, as it allows for the introduction of a variety of residues at specific positions on a polymer chain.[6]

[*] T. G. W. Edwardson, Dr. K. M. M. Carneiro, Dr. C. J. Serpell, Prof. H. F. Sleiman
Department of Chemistry, McGill University
801 Sherbrooke St. West, Montreal, H3A 0B8, Quebec (Canada)
E-mail: christopher.serpell@mcgill.ca
hanadi.sleiman@mcgill.ca
Homepage: http://www.hanadisleiman.com

[**] We are grateful to NSERC, CFI, CSACS, CIHR, and CIFAR for financial support. T.G.W.E thanks CIHR for a DDTP scholarship. C.J.S thanks NSERC for a Banting Postdoctoral Fellowship. H.F.S. is a Cottrell Scholar of the Research Corporation.

Supporting information for this article (including synthetic and purification protocols and additional characterization data) is available on the WWW under http://dx.doi.org/10.1002/anie.201310937.

An alternative method to introduce molecular recognition elements into synthetic polymers is through biomolecule–polymer conjugation,[7] where a conventional synthetic polymer and an information-rich DNA or peptide/protein portion are covalently connected.[8] DNA amphiphiles in particular are especially attractive, because they can self-assemble into a variety of morphologies through microphase separation while retaining the "smart" and addressable biomolecule component;[9] this can result in attractive platforms for functional nucleic acids that can serve as aptamers and silencing RNA,[10] and as membrane anchoring and functionalization tools.[11] However, the synthesis of amphiphilic DNA–polymer conjugates is fundamentally challenging, as it requires the end-to-end coupling of a highly charged DNA strand with a hydrophobic polymer chain. Polymers can be attached to DNA by solid-phase synthesis; however, the yields are suboptimal as these methods and materials are designed for small-molecule attachment.

Herein we report a simple and versatile method for the synthesis of sequence-defined polymers attached to oligonucleotides. Our approach involves the sequential coupling of short, well-defined oligomers to a DNA strand on a solid support. We report the synthesis of monodisperse DNA–polymer conjugates with hydrophilic and hydrophobic units attached to a DNA strand in high yields and complete control over the length and sequence of the monomer units in the final structure.

Scheme 1 illustrates the general synthetic route for DNA–polymer conjugates using phosphoramidite chemistry.[12] In each case, an oligonucleotide of mixed sequence, comprising 19 nucleotides, was first synthesized on the solid support using standard automated procedures (SI-IIIa, Supporting Information (SI)). Next, short oligomers of well-known polymers were appended to the oligonucleotide chain, using the same automated phosphoramidite chemistry.

Initially, we used a commercially available dimethoxytrityl (DMT)-protected dodecanediol phosphoramidite, which corresponds to a hexameric section of poly(ethylene)—referred to as hexaethylene (HE)—for the subsequent coupling steps. The resulting DNA–polymer conjugate would therefore consist of a DNA portion functionalized at its 5′ terminus with a series of HE units punctuated by phosphate moieties. To probe the synthetic limit of the length of these polymeric modifications to the 5′ terminus of the DNA strand, molecules with 1 to 12 successive additions of HE units were first synthesized.

Since the coupling efficiency remains excellent (> 97 %), it is surely possible to generate much longer polymers; however, in this work we chose to stop at twelve units, due to

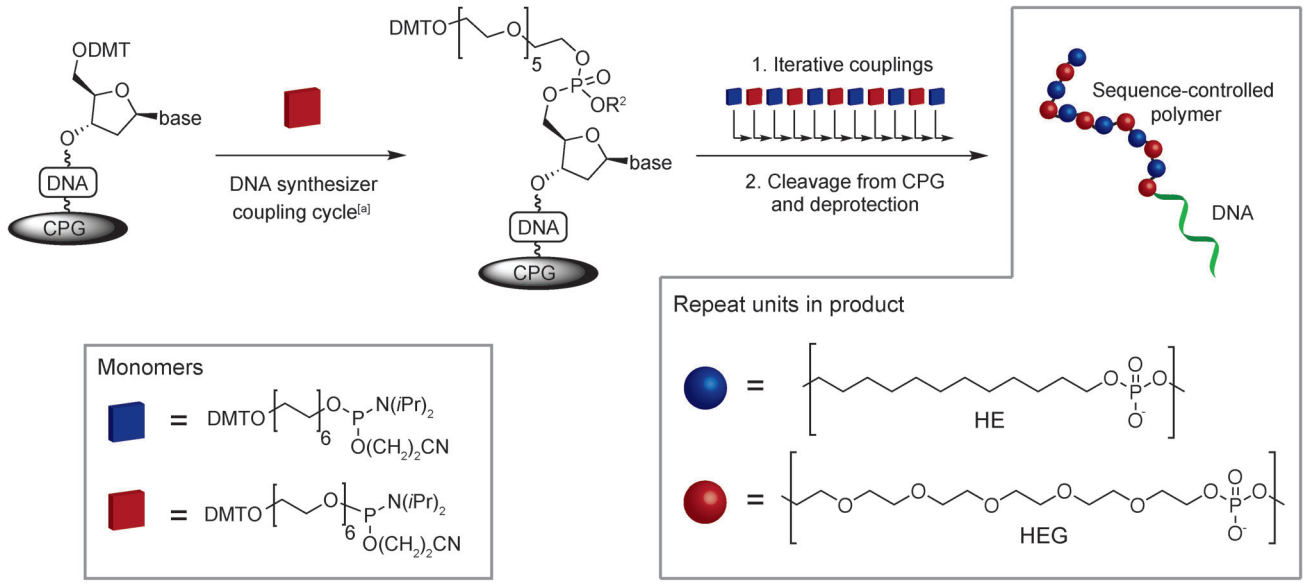

Scheme 1. Synthetic methodology for DNA–polymer conjugates. Monomer phosphoramidites (blue and red squares) are coupled to the 5′ end of the oligonucleotide on the controlled-pore glass support (CPG) in a stepwise fashion. This produces sequence-defined products with repeat units HE and HEG (blue and red spheres). [a] Detailed synthetic protocol can be found in the Supporting Information.

the ease of division into blocks for sequence definition (vide infra). The synthesized block copolymers were cleaved from the solid support and the protecting groups were removed under basic conditions (28% ammonia solution, room temperature, overnight). Analysis of the crude mixtures by reverse-phase HPLC (Figure SF2 (SI)) revealed a narrow product distribution where the target molecule constituted 74–89% of the isolated DNA, a much greater yield than that generally found in couplings of full-length polymers to DNA strands. In the analysis of the products by reverse-phase HPLC (Figure 1) the retention time increased with number of HE blocks, consistent with an increase in hydrophobicity with each HE block added. The identity of the modified oligonucleotides was confirmed by electrospray mass spectrometry (ESI-MS) (Table 1) and matrix-assisted laser desorption ionization mass spectrometry (MALDI-MS) (Table ST3 (SI)).

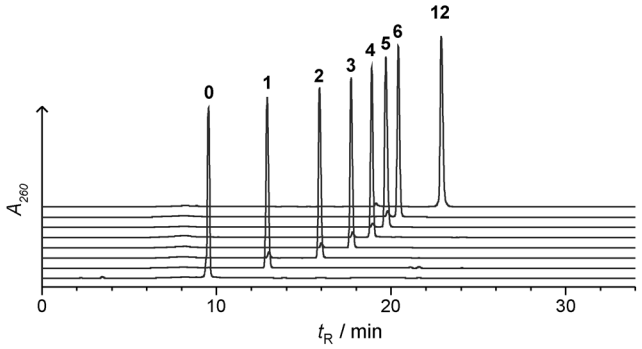

Figure 1. Reverse-phase HPLC traces of purified HE_x–DNA conjugates. Bold numbers above each peak refer to the number of HE units appended to the 5′ terminus of the oligonucleotide. The relationship between number of HE units and retention time is logarithmic (Figure SF2 (SI)).

Table 1: ESI-MS characterization and yields of DNA–HE conjugates.

Conjugate[a]	Product distribution [%][b]	Calculated mass [Da]	Mass found [Da]
HE_1	89	6029.14	6029.13
HE_2	85	6293.29	6293.29
HE_3	86	6557.44	6557.45
HE_4	84	6821.59	6821.61
HE_5	83	7085.74	7085.69
HE_6	83	7349.88	7349.83
HE_{12}	74	8934.78	8934.68

[a] Attached to the 5′ terminus of DNA sequence TTTTTCAGTTGACCA-TATA [b] Percentage of total DNA isolated. See SI-IIIb (SI) for further details.

With the HE_x–DNA molecules characterized, we were interested in the self-assembly behavior of these block-copolymer-like DNA amphiphiles to confirm whether the phosphate-punctuated HE section would behave like a hydrophobic polymer. To probe the self-assembly in solution, dynamic light scattering (DLS) was used to determine the presence and hydrodynamic radius of micellar aggregates. It was found that HE_x–DNA containing five or fewer HE units existed as discrete molecules at a concentration of 10 μM in Mg^{2+}-containing buffer, as indicated by poor scattering intensities (Figure SF7 (SI)). However, for HE_6–DNA, scattering was observed which correlated to a sphere with a hydrodynamic radius (R_h) of 6.5 ± 0.4 nm (Table 2). This size correlates with DNA-based spherical micelles and is consistent with the tight packing of the HE chains in a hydrophobic core surrounded by a charged corona made up of DNA.[9c] Assuming a linear DNA geometry (6.1 nm), this result suggests that the HE_6 chain (1.9 nm per unit if stretched) is folded on itself multiple times and potentially adopts a "concertina" structure analogous to that of phos-

Table 2: ESI-MS characterization and percent yields of sequence-defined HE–HEG polymers.

Conjugate[a]	Product distribution [%][b]	Calculated mass [Da]	Mass found [Da]
$(HE\text{-}HEG)_6$	51	9414.63	9414.60
$(HE_2\text{-}HEG_2)_3$	62	9414.63	9414.58
$(HE_3\text{-}HEG_3)_2$	56	9414.63	9414.58
$HE_6\text{-}HEG_6$	67	9414.63	9414.58
$HEG_6\text{-}HE_6$	78	9414.63	9414.60

[a] Attached to the 5′ terminus of DNA sequence TTTTTCAGTTGACCA-TATA [b] Percentage of total DNA isolated. See SI-IIIb (SI) for further details.

pholipid bilayers. For HE_{12}–DNA under the same conditions $R_h = 11.3 \pm 0.1$ nm, implying that the HE_{12} chain is more extended. The spherical morphology, monodispersity, and relative size of micelles were confirmed by atomic force microscopy (AFM; Figure 2). Thermal and electrophoretic hybridization studies (Figures SF3 and SF6 (SI)) concluded that all of the HE_x–DNA molecules retained their ability to hybridize to a complementary DNA strand, highlighting the orthogonal nature of these modes of intermolecular self-assembly.

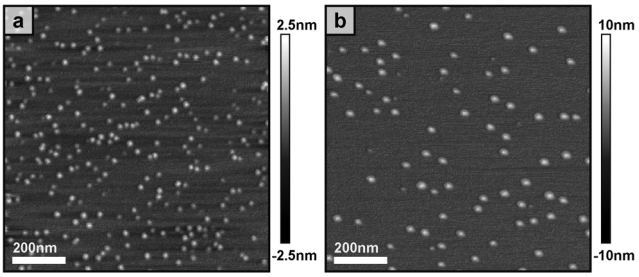

Figure 2. Atomic force microscopy image of a) HE_6–DNA micelles and b) HE_{12}–DNA micelles in air; for details see SI-IVd (SI).

To further show that the behavior of the conjugates was in line with block copolymer assembly, encapsulation of guest molecules within the hydrophobic core of the micelles was performed using Nile Red, a fluorescent dye that displays significant fluorescence in hydrophobic media but negligible emission in aqueous solution.[13] An increase in fluorescence was observed with increasing number of HE units in a 10 μM aqueous solution of the DNA conjugates; the self-assembled macromolecular structure showed the expected dependence on the component molecular structure (Figure 3).

We can therefore conclude that through phosphoramidite coupling, we have produced DNA–poly(ethylene) conjugate mimics in good yields with total control over the degree of polymerization (up to 72 units), leading to molecularly monodisperse products. The presence of phosphate moieties in the polymer backbone does not hinder the hydrophobic properties of the polymer section and spherical micelles capable of encapsulating guests are produced.

Since the stepwise synthesis is inherently sequential, we decided to explore whether a mixed system of hydrophobic

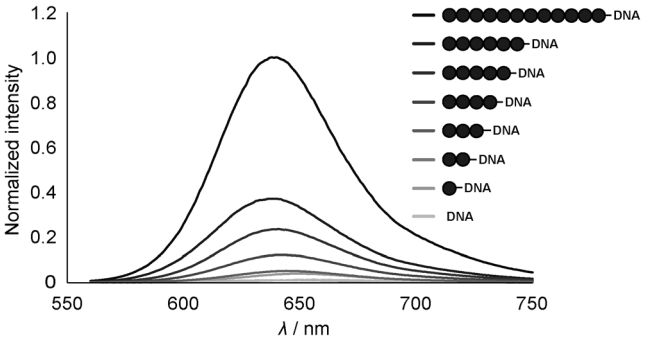

Figure 3. Fluorescence of Nile Red in the presence of 10 μM HE-modified DNA. Dark circles are HE blocks; fluorescence increases with the number of blocks.

HE blocks and hydrophilic hexaethylene glycol blocks (HEG, also available as a commercial DMT-protected phosphoramidite reagent) could be synthesized, and what self-assembly properties the resultant sequence polymers might exhibit. Five different modified oligonucleotides each containing a 5′ modification 12 units in length (six HE, six HEG units) were successfully synthesized. Each of these DNA strands differs in the pattern of the HE and HEG units, which were grouped into blocks of one, two, three, and six oligomers. For the blocks of six oligomers, the position with respect to the DNA was also varied, producing two triblock architectures, HEG_6-HE_6-DNA and HE_6-HEG_6-DNA. These modifications were synthesized under the same conditions as those described for the HE_x–DNA versions and reverse-phase HPLC ascertained that one major product was obtained for all sequences, in contrast to a nonsequenced control (Figure SF1 (SI)). Typically, the best coupling efficiency occurs when the added monomer is the same as the one preceding it. We anticipate that coupling protocols for monomer crossover can be optimized through longer coupling times, increased monomer concentration, and solvent choice. A gradual increase in retention time on the HPLC column was observed as the block size increased from one in $(HE\text{-}HEG)_6$ to six in HE_6-HEG_6 (Figure 4a), indicating a gradual increase in overall hydrophobicity. This may be due to the fact that a minimum number of adjacent HE units are needed to create a hydrophobic pocket that is available for interaction with the stationary phase, whereas hydrophilic groups flanking each HE_x block may diminish strong interactions with the stationary phase.

Another variable in the block pattern that affects the hydrophobic behavior is the position of the HE and HEG blocks with respect to the hydrophilic oligonucleotide; this is evident in the comparison of the molecules HE_6-HEG_6-DNA and HEG_6-HE_6-DNA (Figure 4b). In terms of the amphiphilicity of the different block patterns, HE_6-HEG_6-DNA is a typical amphiphile with a distinct hydrophilic DNA–HEG block and a hydrophobic HE terminus. The bola-amphiphilic HEG_6-HE_6-DNA may adopt a structure in which the oligonucleotide and the HEG blocks provide better shielding of the HE portion from the aqueous medium.

To investigate the effect of block pattern on the amphiphilic self-assembly in solution, DLS measurements were

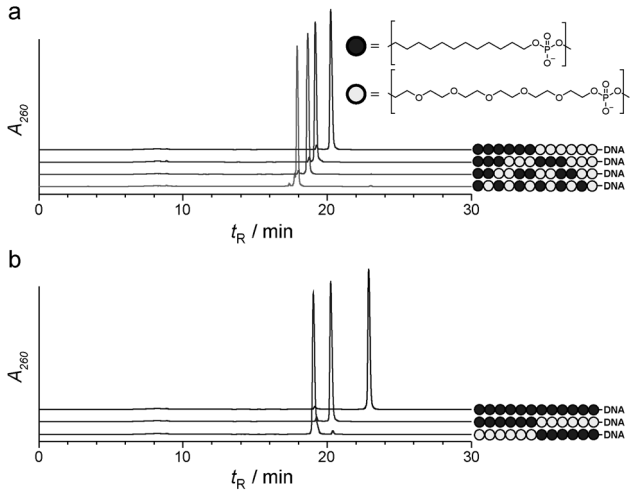

Figure 4. Reverse-phase HPLC traces of sequence-defined HE-HEG polymers. a) HE/HEG block sizes from 1 to 6. b) HE/HEG block positions for HE_6-HEG_6-DNA and HEG_6-HE_6-DNA with respect to the DNA portion.

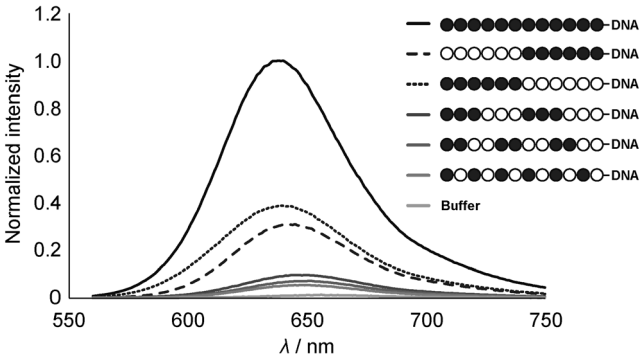

Figure 5. Fluorescence of Nile Red in the presence of 10 μM HE/HEG-sequenced modifications. Increasing intensity is observed with increasing block size. Filled circles: hydrophobic HE; empty circles: hydrophilic HEG.

carried out for the HE/HEG series. We found that the trends in hydrophobicity observed by HPLC were amplified under self-assembly conditions. The strands with polymer sequences $(HE\text{-}HEG)_6$, $(HE_2\text{-}HEG_2)_3$, and $(HE_3\text{-}HEG_3)_2$ did not exhibit self-assembly at this concentration (10 μM). However, strong scattering was seen for HE_6-HEG_6-DNA with an associated R_h of 9.7 ± 0.9 nm, although not for HEG_6-HE_6-DNA. AFM characterization was also attempted for HE_6-HEG_6-DNA but was less conclusive than for the HE system; this is likely due to different surface adsorption properties which may be mediated by the addition of HEG blocks (SI-IVd (SI)). Firstly, the DLS observations lend further weight to the hypothesis that a minimum block size of HE_6 is required for significant hydrophobic character to be exhibited. Furthermore, the effect of the positioning of the blocks with respect to the oligonucleotide portion is also a major factor in the self-assembly: the terminal HE_6 block results in micellization, whereas a central HE_6 block prevents aggregation. Thermal and electrophoretic hybridization experiments confirmed the availability of the DNA (Figures SF3 and SF6 (SI)).

The sequence-specific self-assembly was also assessed using the encapsulation of Nile Red (Figure 5). In this case a small increase in fluorescence was seen as the block size increased from one to three HE units. This is consistent with a degree of intramolecular collapse of adjacent HE units, such that progressively larger hydrophobic domains are generated as the block size increases. At a block size of six, both of the DNA-sequence polymers displayed a similar level of Nile Red fluorescence, although that of HEG_6-HE_6-DNA was slightly lower. A small, but reproducible, red shift of the maximum emission from the bola-amphiphile (640 nm) with respect to the linear amphiphile (645 nm) was also observed, which indicates that Nile Red is in a more polar environment.[14] This is consistent with an intermolecular spherical micelle being formed by HE_6-HEG_6-DNA, and an intramolecular hydrophobic domain being formed in HEG_6-HE_6-DNA, resulting in a lower volume-to-surface area ratio and greater exposure of the dye to the solvent.

Finally the reversibility of the self-assembly process was investigated using DLS. It was found that the presence of Mg^{2+} ions was required for micelle formation and could be used to "switch on" and "off" the aggregation. Upon addition of Mg^{2+} to a solution of discrete HE_6-DNA, HE_{12}-DNA, or HE_6-HEG_6-DNA strands, assembly was observed by DLS within 45 seconds. Furthermore, addition of EDTA to sequester Mg^{2+} ions was found to cause deaggregation within 30 seconds. In both cases, the nonassembling sequence HEG_6-HE_6-DNA showed no change (Figures SF8–SF10 (SI)).

In conclusion, we have demonstrated a facile and high-yielding procedure for the production of monodisperse amphiphilic DNA block copolymers using standard automated techniques and commercially available materials. Such materials have been previously extremely difficult to obtain in good purity and yield, and with reliable characterization. Secondly, we have further shown that the same procedure can easily be used to create synthetic sequence-defined polymers, and that the variation in the overall hydrophobicity, self-assembly, and encapsulation properties can be logically altered by variation of the sequence. Control of sequence-specific hydrophobic intra- or intermolecular aggregation within a polymer is an important result: the same process is a major determinant of protein folding, and by mirroring that assembly here, the stage is set for synthetic mimics of the complex structures and functions exhibited by biological sequenced polymers.[15] The methods reported are accessible to any researcher with the capacity for oligonucleotide synthesis, and in principle the scope extends far beyond the HE and HEG components used here—other diols can be converted into a DMT-phosphoramidite reagent and used similarly. Importantly, many functional groups, such as amides, aryl halides, ethers, disulfides, maleimides, alkenes, alkynes, and protected amines are compatible with phosphoramidite coupling. Oligonucleotide strands of up to 100 additions can typically be produced with standard equipment, and since the coupling efficiency is excellent, similar maximum lengths can be expected. This synthetic method has the potential to produce new oligonucleotide conjugates for use

in therapeutics and as supramolecular foldamers or simple protein mimics for the study of complex self-assembly mediated by hydrophobic and other supramolecular interactions.

Received: December 17, 2013
Published online: March 26, 2014

Keywords: amphiphiles · DNA · polymers · self-assembly · solid-phase synthesis

[1] J.-F. Lutz, M. Ouchi, D. R. Liu, M. Sawamoto, *Science* **2013**, *341*, 1238149.
[2] a) J.-F. Lutz, *Acc. Chem. Res.* **2013**, *46*, 2696 – 2705; b) S. Pfeifer, J.-F. Lutz, *J. Am. Chem. Soc.* **2007**, *129*, 9542 – 9543; c) D. Benoit, C. J. Hawker, E. E. Huang, Z. Lin, T. P. Russell, *Macromolecules* **2000**, *33*, 1505 – 1507; d) M. Minoda, M. Sawamoto, T. Higashimura, *Macromolecules* **1990**, *23*, 4889 – 4895.
[3] a) R. B. Merrifield, *J. Am. Chem. Soc.* **1963**, *85*, 2149 – 2154; b) R. L. Letsinger, V. Mahadevan, *J. Am. Chem. Soc.* **1965**, *87*, 3526 – 3527.
[4] a) P. J. Milnes, M. L. McKee, J. Bath, L. Song, E. Stulz, A. J. Turberfield, R. K. O'Reilly, *Chem. Commun.* **2012**, *48*, 5614 – 5616; b) J. Niu, R. Hili, D. R. Liu, *Nat. Chem.* **2013**, *5*, 282 – 292.
[5] a) B. Lewandowski, G. De Bo, J. W. Ward, M. Papmeyer, S. Kuschel, M. J. Aldegunde, P. M. E. Gramlich, D. Heckmann, S. M. Goldup, D. M. D'Souza, A. E. Fernandes, D. A. Leigh, *Science* **2013**, *339*, 189 – 193; b) G. Gody, T. Maschmeyer, P. B. Zetterlund, S. Perrier, *Nat. Commun.* **2013**, *4*, 2505.
[6] D. Schaffert, C. Troiber, E. E. Salcher, T. Fröhlich, I. Martin, N. Badgujar, C. Dohmen, D. Edinger, R. Kläger, G. Maiwald, K. Farkasova, S. Seeber, K. Jahn-Hofmann, P. Hadwiger, E. Wagner, *Angew. Chem.* **2011**, *123*, 9149 – 9152; *Angew. Chem. Int. Ed.* **2011**, *50*, 8986 – 8989.
[7] M. Kwak, A. Herrmann, *Chem. Soc. Rev.* **2011**, *40*, 5745 – 5755.
[8] J. Y. Shu, B. Panganiban, T. Xu, *Annu. Rev. Phys. Chem.* **2013**, *64*, 631 – 657.
[9] a) M.-P. Chien, A. M. Rush, M. P. Thompson, N. C. Gianneschi, *Angew. Chem.* **2010**, *122*, 5202 – 5206; *Angew. Chem. Int. Ed.* **2010**, *49*, 5076 – 5080; b) O. Pokholenko, A. Gissot, B. Vialet, K. Bathany, A. Thiery, P. Barthelemy, *J. Mater. Chem. B* **2013**, *1*, 5329 – 5334; c) L. Wang, Y. Feng, Z. Yang, Y.-M. He, Q.-H. Fan, D. Liu, *Chem. Commun.* **2012**, *48*, 3715 – 3717; d) K. M. M. Carneiro, G. D. Hamblin, K. D. Hanni, J. Fakhoury, M. K. Nayak, G. Rizis, C. K. McLaughlin, H. S. Bazzi, H. F. Sleiman, *Chem. Sci.* **2012**, *3*, 1980 – 1986; e) T. G. W. Edwardson, K. M. M. Carneiro, C. K. McLaughlin, C. J. Serpell, H. F. Sleiman, *Nat. Chem.* **2013**, *5*, 868 – 875.
[10] a) Y. Wu, K. Sefah, H. Liu, R. Wang, W. Tan, *Proc. Natl. Acad. Sci. USA* **2010**, *107*, 5 – 10; b) M. Raouane, D. Desmaële, G. Urbinati, L. Massaad-Massade, P. Couvreur, *Bioconjugate Chem.* **2012**, *23*, 1091 – 1104.
[11] a) J. G. Woller, J. K. Hannestad, B. Albinsson, *J. Am. Chem. Soc.* **2013**, *135*, 2759 – 2768; b) E. P. Lundberg, B. Feng, A. Saeid Mohammadi, L. M. Wilhelmsson, B. Nordén, *Langmuir* **2012**, *28*, 285 – 293; c) Y.-H. Chan, B. Lengerich, S. Boxer, *Biointerphases* **2008**, *3*, FA17 – FA21.
[12] S. L. Beaucage, M. H. Caruthers, *Tetrahedron Lett.* **1981**, *22*, 1859 – 1862.
[13] P. Greenspan, E. P. Mayer, S. D. Fowler, *J. Cell Biol.* **1985**, *100*, 965 – 973.
[14] P. Greenspan, S. D. Fowler, *J. Lipid Res.* **1985**, *26*, 781 – 789.
[15] a) J. C. M. van Hest, D. A. Tirrell, *Chem. Commun.* **2001**, 1897 – 1904; b) O. Altintas, C. Barner-Kowollik, *Macromol. Rapid Commun.* **2012**, *33*, 958 – 971.

